BJCP British Journal of Clinical Pharmacology

DOI:10.1111/bcp.12426

Population pharmacokinetic–pharmacodynamic modelling of mycophenolic acid in paediatric renal transplant recipients in the early post-transplant period

Min Dong,[1]* Tsuyoshi Fukuda,[1,3]* Shareen Cox,[1] Marij T. de Vries,[1] David K. Hooper,[2,3] Jens Goebel[2,3] & Alexander A. Vinks[1,3]

Divisions of [1]Clinical Pharmacology and [2]Nephrology and Hypertension, Cincinnati Children's Hospital Medical Center and [3]Department of Pediatrics, University of Cincinnati College of Medicine, Cincinnati, OH, USA

Correspondence
Professor Alexander A. Vinks PharmD PhD, Division of Clinical Pharmacology, Cincinnati Children's Hospital Medical Center, 3333 Burnet Avenue, MLC 6018, Cincinnati, OH 45229-3039, USA.
Tel.: +1 513 636 0159
Fax: +1 513 636 4402
E-mail: sander.vinks@cchmc.org

*The first two authors contributed to this work equally.

Keywords
inosine monophosphate dehydrogenase (IMPDH), mycophenolic acid, paediatric patient, pharmacodynamics, pharmacokinetics, transit absorption model

Received
5 July 2013

Accepted
12 May 2014

Accepted Article Published Online
16 May 2014

WHAT IS ALREADY KNOWN ABOUT THIS SUBJECT

- Mycophenolic acid (MPA) exhibits wide between and within patient pharmacokinetic (PK) variability. Efforts have been dedicated to the development of individualized dosing strategies, but the complex PK of MPA have partly hampered efficient use of PK assisted dosing.
- Inosine monophosphate dehydrogenase (IMPDH) is the molecular target of MPA. Monitoring IMPDH activity may represent an attractive strategy to tailor immunosuppression to individual needs.

WHAT THIS STUDY ADDS

- An integrated population pharmacokinetic–pharmacodynamic (PK–PD) model was developed to describe simultaneously the relationship between MPA dose, MPA plasma concentration and IMPDH inhibition in paediatric kidney transplant patients.
- Although prospective evaluation is needed, targeting IMPDH inhibition as a surrogate PD marker of MPA induced immunosuppression, when used in an integrated PK–PD fashion, may provide a better predictor of clinical outcome. The developed population PK–PD model may be used to establish a Bayesian algorithm to allow PK–PD guided personalized dosing.

AIM

The purpose of this study was to develop a population pharmacokinetic and pharmacodynamic (PK–PD) model for mycophenolic acid (MPA) in paediatric renal transplant recipients in the early post-transplant period.

METHODS

A total of 214 MPA plasma concentrations–time data points from 24 patients were available for PK model development. In 17 out of a total of 24 patients, inosine monophosphate dehydrogenase (IMPDH) enzyme activity measurements ($n = 97$) in peripheral blood mononuclear cells were available for PK–PD modelling. The PK–PD model was developed using non-linear mixed effects modelling sequentially by 1) developing a population PK model and 2) incorporating IMPDH activity into a PK–PD model using *post hoc* Bayesian PK parameter estimates. Covariate analysis included patient demographics, co-medication and clinical laboratory data. Non-parametric bootstrapping and prediction-corrected visual predictive checks were performed to evaluate the final models.

RESULTS

A two compartment model with a transit compartment absorption best described MPA PK. A non-linear relationship between dose and MPA exposure was observed and was described by a power function in the model. The final population PK parameter estimates (and their 95% confidence intervals) were CL/*F*, 22 (14.8, 25.2) l h^{-1} 70 kg^{-1}; V_c/F, 45.4 (29.6, 55.6) l; V_p/F, 411 (152.6, 1472.6)l; Q/*F*, 22.4 (16.0, 32.5) l h^{-1}; K_a, 2.5 (1.45, 4.93) h^{-1}. Covariate analysis in the PK study identified body weight to be significantly correlated with CL/*F*. A simplified inhibitory E_{max} model adequately described the relationship between MPA concentration and IMPDH activity. The final population PK–PD parameter estimates (and their 95% confidence intervals) were: E_0, 3.45 (2.61, 4.56) nmol h^{-1} mg^{-1} protein and EC_{50}, 1.73 (1.16, 3.01) mg l^{-1}. E_{max} was fixed to 0. There were two African-American patients in our study cohorts and both had low IMPDH baseline activities (E_0) compared with Caucasian patients (mean value 2.13 mg l^{-1} *vs.* 3.86 mg l^{-1}).

CONCLUSION

An integrated population PK–PD model of MPA has been developed in paediatric renal transplant recipients. The current model provides information that will facilitate future studies and may be implemented in a Bayesian algorithm to allow a PK–PD guided therapeutic drug monitoring strategy.

Introduction

Mycophenolic acid (MPA), the active moiety of mycophenolate mofetil (MMF, CellCept®), is the most commonly used immunosuppressant in paediatric renal transplant recipients [1]. MPA exhibits its main effect by inhibiting inosine monophosphate dehydrogenase (IMPDH), the key enzyme in the *de novo* purine synthesis pathway in T and B lymphocytes. Our group, along with others, has demonstrated that IMPDH enzyme activity is a reliable pharmacodynamic (PD) biomarker for the MPA effect in adult and in paediatric kidney transplant recipients [2–4].

Although the effectiveness of MPA to prevent acute rejection in solid organ transplantation has been broadly recognized, the large inter- and intra-individual variability in drug disposition provides a big challenge for tailoring the MPA dose to individual needs. Prospective randomized studies demonstrated that therapeutic drug monitoring (TDM) and targeting MPA exposure (AUC(0,12 h) of 30–60 mg l^{-1} h) can improve patient outcome [5], especially in those patients who have high immunologic risk [6]. A great amount of effort has been dedicated to the development of population pharmacokinetic (PK) models to predict MPA disposition in adult and paediatric kidney transplant recipients. Demographic and physiological covariates such as body weight, estimated creatinine clearance and total bilirubin have been identified to explain part of the inter-individual variability [7–9]. Based on population PK studies, several Bayesian estimators have been developed and allow the estimation of MPA exposure based on sparse optimally sampled TDM data [10]. To date, individualization of MPA therapy has been predominantly focused on optimization through targeting PK. Yet, with the current acute rejection incidence in paediatric renal transplant recipients still at 15 to 35%, there is an important clinical need for better therapeutic management strategies [6]. Since IMPDH is the molecular target of MPA, IMPDH activity may serve as a better biomarker for immunosuppression and clinical response. By monitoring MPA-induced IMPDH inhibition, not only the drug exposure, but the inter-individual variability in response to the drug will be taken into account, resulting in a more accurate prediction of therapeutic effect rather than what can be achieved by monitoring of MPA plasma concentrations alone [4, 11]. The objective of the current study was to develop a PK–PD population model to describe simultaneously the MPA PK and IMPDH data in paediatric kidney transplant recipients.

Methods

Patients

Data came from paediatric kidney transplant patients participating in a prospective multicentre clinical study as previously described [3]. A total of 214 MPA plasma concentration–time data points from 24 patients were available for PK analysis. IMPDH activity measurements ($n = 97$) were available in 17 out of the total 24 patients. Demographic data collected included age, gender, weight, height and race. Estimated lean body weight (eLBW) and normalized body weights were calculated based on the methods described by Peters *et al*. [12] and Duffull *et al*. [13], respectively. Body mass index (BMI) was calculated using the standard formula: weight (kg)/[height (m)]^2. A BMI equal to or greater than the 95th percentile on the CDC BMI-for-age growth charts for girls and boys was considered as obese. Creatinine clearance (CL_{cr}) was calculated based on serum creatinine concentration by the Schwartz formula [14]. Other medical information such as concomitant medications was collected by reviewing patients' medical records. Patient demographics are summarized in Table 1.

Immunosuppressive therapy

Patients were started pre-surgery on 450 or 600 mg m^{-2} of MMF (CellCept®) twice a day according to each institutional protocol. Subsequent dose adjustments were based on clinical status and at the discretion of the prescribing physician. All other immunosuppressive therapy was initiated directly following the transplant surgery. Basiliximab (Simulect) or rabbit antithymocyte globulin (Thymoglobulin) was used as induction immunosuppression therapy in all patients. Tacrolimus was dosed twice daily to obtain the following trough concentrations: 15 μg l^{-1} (first 2 weeks), 12 μg l^{-1} (weeks 3–6), 10 μg l^{-1} (weeks 7–10), 7–10 μg l^{-1} (weeks 11–12) and 6–8 μg l^{-1} (month 4 and further). The initial dose of prednisone was 1.0–1.5 mg kg^{-1} twice daily; and subsequently tapered at the treating physician's discretion. Patients on concomitant cyclosporin were excluded from the study. The study was approved by the institutional review boards (IRB) of the participating institutions. All patients or parents/guardians provided written informed consent or assent (age 12 to <18 years) before enrolment in the study.

PK–PD sampling

On days 4–9 post-transplantation, blood samples for PK and biomarker measurements were collected at pre-dose, and at 20 min, 40 min, 1, 1.5, 2, 3, 4, 6 and 9 h after oral MMF administration. For patients weighing less than 15 kg, a less intense sampling schedule was used: pre-dose, 30 min, 1, 2, 4, 6 and 9 h after the morning MMF dose. This reduced sampling schedule was utilized because of restrictions on the maximum blood draw volume in these patients. A blood sample was obtained prior to transplant to provide pre-transplant baseline IMPDH activity.

PK and IMPDH assays

MPA was measured as previously described [3]. Briefly, plasma MPA concentrations were analyzed using solid

Table 1
Patients demographics

	PK study ($n = 24$)		PK–PD study ($n = 17$)	
	Mean (Median)	Range	Mean (Median)	Range
Age (years)	12.1 (14.2)	2.1–20.2	13.4 (14.7)	4.1–20.2
Weight (kg)	39.8 (38.2)	10.3–106.4	43.5 (43.3)	10.3–106.0
Height (cm)	137.3 (143.1)	81.2–174.0	142.6 (154.0)	83.0–171.0
Body Surface Area (BSA) (m^2)	1.21 (1.26)	0.49–2.21	1.3 (1.4)	0.49–2.21
Dose/BSA (mg m^{-2})	444.4 (444.0)	244.6–589.6	427.0 (430.0)	244.6–589.6
Creatinine Clearance (ml min^{-1} 1.73 m^{-2})	118.1 (111.4)	20.5–228.3	114.6 (111.0)	20.5–228.0
Albumin (g dl^{-1})	3.5 (3.5)	2.1–4.7	3.4 (3.5)	2.1–4.4
HGB (g dl^{-1})	10.8 (10.7)	7.6–14.4	10.9 (10.7)	7.6–14.4
Gender	Number of patients	Percentage (%)	Number of patients	Percentage (%)
Male/Female	15/9	62.5/37.5	10/7	58.8/41.2
Race				
Caucasian/African	20/4	83/17	15/2	88.2/11.8

phase extraction and a validated high performance liquid chromatography (HPLC) assay. Intra- and inter-day coefficients of variation were below 5%. The lower limit of quantification (LLOQ) for MPA was 0.25 mg l^{-1}. IMPDH activity in mononuclear cells (MNCs) was determined according to the method described by Glander *et al.* [15] and by Fukuda *et al.* [3]. Xanthosine 5′-monophosphate (XMP) and intracellular adenosine 5′-monophosphate (AMP) were measured by validated HPLC assay in MNCs lysate after incubation with inosine 5′-monophosphate (IMP). The LLOQ for both XMP and AMP was 90 pmol/sample. Intra- and inter-day coefficients of variation for XMP and AMP quality control samples were below 7% throughout. IMPDH activity was expressed as the ratio of XMP and AMP as well as produced XMP per time unit per mg protein.

The area under the curve (AUC) for each subject over the time interval for plasma concentration was computed by Phoenix WinNonlin® (version 6.2.1).

Population PK–PD modelling

Population PK–PD analysis was conducted using NONMEM version 7.2.0 (ICON, Ellicott City, MD, USA) on a 64-bit Linux Operation System with an Intel Fortran Compiler (v 12.0). PDx-Pop (version 5, ICON, Ellicott City, MD, USA) was used as the graphical user interface for running NONMEM and for processing NONMEM output. Visualization of NONMEM output was implemented by Xpose 4 package in R (v 2.15.0.). First order conditional estimation with interaction (FOCE-I) was employed throughout to estimate simultaneously the typical population PK parameters, random effect of inter-individual variability and residual errors. Model structure selection was based on goodness-of-fit criteria, including convergence with at least three significant digits, diagnostic plots, physiological plausibility of the parameter estimates and Akaike Information Criterion (AIC). Inter-individual variability (IIV) was modelled using an exponential model which assumed a normally distributed inter-individual variable with a mean of zero and a variance of ω^2 (equation 1):

$$P_i = P_{TV} * e^{\eta i} \quad (1)$$

where P_i is the parameter estimate for the i^{th} individual subject; P_{TV} is the typical population value of the parameter P and η_i is the inter-individual random effects for individual i. For the PK analysis, models were fitted to log transformed data using an additive error model. For the PK–PD residual unexplained variability, an additive, a proportional or a combined (additive and proportional) model (equation 2) was considered:

$$C_{ij} = C_{pred,ij} + C_{pred,ij} * \varepsilon_{prop,ij} + \varepsilon_{add,ij} \quad (2)$$

where C_{ij} represents the jth observed value of the dependent variables in individual i, $C_{pred,ij}$ is the jth model predicted values of the dependent variables in individual i and $\varepsilon_{prop,ij}$ and $\varepsilon_{add,ij}$ are the proportional and additive residual random errors, respectively.

Demographic and laboratory characteristics of the patients including age, height, gender, race, estimated creatinine clearance, albumin and co-medication were screened as potential covariates using a stepwise selection method. For any covariate that had missing values in more than 10% of the patients, that covariate was not included in the analysis. Otherwise, missing covariates were imputed with median value of remaining values. The change in the objective function value (OFV) between two nested models was assumed to follow the χ^2 distribution. A reduction of OFV by 3.84 ($P < 0.05$) for forward inclusion and an increase of OFV by 6.64 ($P < 0.01$) for backward elimination were the criteria for retaining a covariate in the model. Power models were applied for both continuous

covariates (equation 3) and categorical covariates (equation 4):

$$P = P_{TV} * (CON_i / CON_{ref}) \wedge \theta_{CON} \quad (3)$$

$$P = P_{TV} * \theta_{CAT} \wedge CAT_i \quad (4)$$

where P is the parameter estimation, P_{TV} is the parameter when the covariate is equal to the reference covariate value, CON_i is the value of the continuous covariate CON in the individual i, CON_{ref} is a reference value for the covariate, θ_{CON} and θ_{CAT} are the estimated parameters describing the magnitude of the covariate–parameter relationships and CAT_i is the value of the categorical covariate CAT in the individual i.

To describe the drug non-proportionality observed in this study, a power function was applied where the relationship between PK parameters and MMF dose was estimated as shown in equation 5.

$$BIO = BIO_{TV} * (DBSA_i / 450) \wedge \theta_{dose} \quad (5)$$

in which BIO_{TV} was the bioavailability if patients received 450 mg m^{-2} of MMF and was arbitrarily fixed to the value of 1, $DBSA_i$ was the dose per body surface area in the individual i and θ_{dose} was an estimated exponent describing the shape of the relationship.

As MPA absorption was found to be highly variable upon initial visual inspection, different absorption models were compared: 1) a first order absorption with or without a lag time (ADVAN4, TRANS4 subroutine), 2) a zero order with or without a lag time (ADVAN3, TRANS4 subroutine), 3) a Weibull-type absorption model (ADVAN6, TOL = 6), 4) a sequential linked or unlinked zero order and first order absorption [16] (ADVAN6, TOL = 6), and 5) a transit compartment model (ADVAN6, TOL = 6). The transit absorption model, first proposed by Savic & Karlsson [17] for single doses, was later extended for multiple doses [18]. It was found to have advantages over pure empirical absorption models for describing atypical absorption profiles. This semi-mechanistic model describes the absorption as a process of drug travelling through a number of hypothetical transit compartments. The optimal number of the compartments and the transit time between compartments were estimated using equation 6.

$$\frac{dA}{dt} = dose \cdot k_{tr} \cdot \frac{(k_{tr} * tad)^n \cdot e^{-k_{tr} * tad}}{\Gamma(n)} \quad (6)$$

where dA/dt is the change of the drug in the absorption compartment, k_{tr} is a transit rate constant; tad is the time after the last dose and n is the number of transit compartment. $\Gamma(n)$ is the gamma function which was numerically transformed using the Stirling approximation.

$$\Gamma(n) = \sqrt{2\pi} \cdot n^{n+0.5} \cdot e^{-n} \quad (7)$$

For the population PK–PD analysis, individual PK parameter estimates from *post hoc* Bayesian estimation were used to describe IMPDH activity. Based on visual inspection and previous preliminary analysis [3], the relationship between MPA concentration (C) and IMPDH activity (E) was modelled with an inhibitory E_{max} model as follows:

$$E = E_0 - \frac{(E_0 - E_{max}) * C}{EC_{50} + C} \quad (8)$$

where E_0 is the baseline IMPDH activity (i.e. with no MPA present ($C = 0$)), E_{max} is the maximal inhibitory effect and EC_{50} is the MPA concentration at half E_{max}.

Model validation

For quality evaluations, non-parametric bootstrap analyses were run using Perl-speaks-NONMEM (PsN) [19]. The original dataset was resampled with 300 replicate data sets and the estimated means and 95% confidence intervals (CIs) of parameter estimates from the bootstrap analysis were compared with the final model estimates. The final models were further evaluated by prediction-corrected visual predictive check (pcVPC) implemented in PsN [20]. One thousand replicates of simulated dataset were generated using the final models and the real data observations were compared with the distribution of simulated concentrations. Also, the shrinkage for inter-individual variability and residual errors was calculated for diagnostic assessment [21].

Results

Population PK modelling

Of the 214 MPA plasma concentration measurements, none was reported to be below LLOQ. A two compartment structural model better described the data than a one compartment model. Since no reference intravenous data were available, the base model was parameterized as apparent clearance (CL/F, l h^{-1}), apparent volume of distribution (central = V_c/F, peripheral = V_p/F, l), apparent intercompartmental clearance (Q/F, l h^{-1}), and first order absorption rate constant (K_a, h^{-1}). A three compartment model was also considered but did not provide additional advantage over the two compartment model. For the absorption phase, a transit compartment model showed the best fit among tested absorption models based on graphical diagnostics, AIC and value of inter-individual

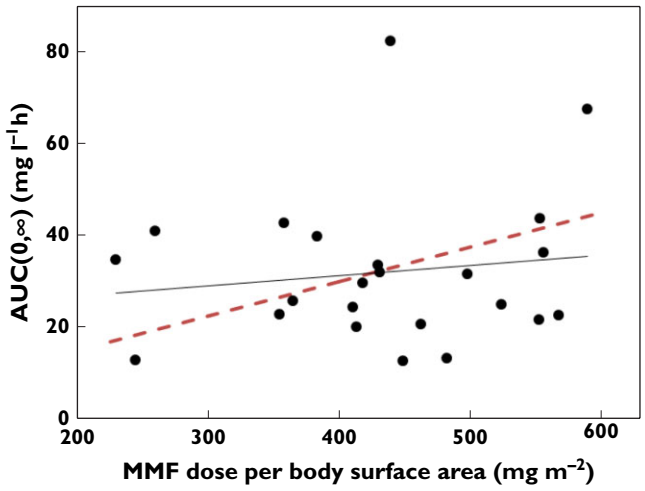

Figure 1

Area under the curve zero to infinity (AUC(0,∞)) *vs.* administered MMF dose per DBSA. The grey line represents the linear regression between the AUC and dose. The red dashed line represents a projected line based upon drug proportionality principle

variability estimates. Due to numerical complexity, the number of transit compartments was fixed to eight based on our previous study [22] and based on interactive visualization of the model output. Removal of inter-individual variability on V_c/F, V_p/F and Q/*F* provided more stable models and did not significantly compromise the model fit and therefore they were fixed to 'zero' during the model-building process. A non-proportional relationship between MPA exposure and dose was observed (Figure 1) which was described by equation 5 with an estimated exponent of −0.43, consistent with a previously reported value of −0.41 in adult patients [23]. Of the covariates tested, inclusion of body weight was found to have a significant influence on CL/*F* ($\Delta OFV = -7.05$, $P < 0.01$). In the study population, three out of 24 patients were obese as defined by a BMI equal to or greater than the 95th percentile on the CDC BMI-for-age growth charts. To evaluate the influence of fat mass, estimated lean body weight and normalized body weight were tested in the covariate analysis, but both covariates did not provide a better fit than when using total body weight. Other tested covariates included age, gender, race, creatinine clearance, albumin, co-medication of thymoglobulin and co-medication of basiliximab. However, none of them significantly improved the model.

Final PK parameter estimates, inter-individual variability and residual variability are presented in Table 2. The mean population PK parameter estimations in our study were CL/*F* 22.0 l h^{-1}/70 kg, V_c/F 45.4 l, Q/*F* 22.4 l h^{-1}, V_p/F 411 l and K_a 2.5 h^{-1}. Goodness-of-fit plots did not show systematic bias for the PK model predictions (Figure 2). Median values and 95% CIs from bootstrap analysis were listed in Table 2. All model parameter estimates were within the 95% CIs and deviated less than 10% from the median value obtained by the bootstrap analysis, indicating the stability of the model. In addition to non-parametric bootstrap analysis, the final PK model was also evaluated by prediction-corrected visual predictive check (pcVPC). As shown in Figure 3, the median, 5% percentile and 95% percentile prediction interval were in good agreement with observed data.

Population PK–PD modelling

All IMPDH activity measurements were above LLOQ. For PK–PD modelling, sequential and simultaneous modelling were both implemented but the sequential method provided more stable estimates and this method was therefore used in the final modelling process. *Post hoc* Bayesian PK parameter estimates for each individual were incorporated into the PK-PD model to link with IMPDH activity. The relationship between IMPDH activity and MPA plasma concentration was adequately modelled by an inhibitory E_{max} model. However, the parameter E_{max} was not reliably estimated (RSE >50%) and was fixed to 0. Only proportional residual error was included in the final model given that the model was not improved by including additive residual error. Interestingly, the two African-American patients had a low baseline IMPDH activity (E_0) (mean value 2.13 mg l^{-1} *vs.* 3.86 mg l^{-1} in Caucasian) and including race as a covariate of E_0 significantly decreased OFV ($\Delta OFV = -8.84$). However, the 95% CI of −1.09 to +0.50 in the bootstrap analysis indicated unreliable covariate effect of race. Consequently, race was not included in our final model. We also found a positive correlation between albumin concentration and IMPDH baseline activity but this correlation did not meet the required significance level ($\Delta OFV = -4.26$, $P > 0.01$) and was therefore not included in the final model. Despite the relative high EC_{50} η-shrinkage (26%), no influential covariates could be identified, suggesting that the available data may not be sufficiently informative for covariate identification for this parameter. For model diagnosis, goodness-of-fit plots did not indicate a systematic bias for the final PK–PD model predictions (Figure 4). The results of the final model and bootstrap procedure are summarized in Table 3. The main PD parameter estimates in our study were E_0 3.45 nmol h^{-1} mg^{-1} protein and EC_{50} 1.73 mg l^{-1}. pcVPC results indicated that the final model adequately described the IMPDH data (Figure 5). Median parameter estimates and 95% CIs from bootstrap analysis showed no obvious systematic bias from the estimates in the final PK–PD model.

Discussion

In this study, an integrated PK–PD model of MPA was developed to describe simultaneously the relationship between MPA dose, MPA plasma concentration and

Table 2

Parameter estimates from the final PK model and bootstrap analysis

Parameters	Final estimates	Shrinkage (%)	Bootstrap estimates†	
			Median	95% CI
CL/*F* (l·h^{-1}·70 kg^{-1})*				
CL/*F* = θ_1 * (body weight/70)$^{\theta 2}$				
θ_1	22.0		21.5	14.8, 25.2
θ_2	0.31		0.31	0.03, 0.63
V_c/*F* (l)	45.4		43.3	29.6, 55.6
Q/*F* (l·h^{-1})	22.4		23.1	16.0, 32.5
V_p/*F* (l)	411		410.6	152.6, 1472.6
K_a (h^{-1})	2.5		2.7	1.45, 4.93
MTT (h)	0.25		0.25	0.12, 0.50
Number of transit compartment (n)	8 fix		–	–
Relative biovailability				
BIO = θ_3 * (DBSA/450)$^{\theta 4}$				
θ_3	1 fix		–	–
θ_4	–0.43		–0.44	–1.00, –0.06
Inter-individual variability (%CV)‡				
ω (CL/*F*)	25.9	15%	24.8	8.1, 38.5
ω (V_c/*F*)	0 fix		–	–
ω (Q/*F*)	0 fix		–	–
ω (V_p/*F*)	0 fix		–	–
ω (K_a)	299.6	29%	288.4	123.6, 910.8
ω (MTT)	144.8	34%	148.5	69.4, 414.1
ω (*n*)	0 fix		–	–
Additive residual error (%CV)[c]				
$\sigma^{additive}$	51.0	10%	50.0	43.5, 57.1

*Apparent clearance is normalized by a reference body weight of 70 kg. †Obtained from 285 out of 300 non-parametric bootstrap runs. ‡Reported as %CV, calculated by the equation 100*SQRT(exp(ω_n) – 1) where ω_n is the NONMEM output for the inter-subject variability of the nth parameter. [c]Calculated by the equation 100 × SQRT(σ), where σ is the NONMEM output for the variance of the additive residual error. %CV, coefficient of variation; BIO, relative bioavailability; CI, confidence interval; CL/*F*, apparent clearance; DBSA, dose per body surface area; K_a, absorption rate constant; MTT, mean transit time; Q/*F*, apparent compartmental clearance between V_c/*F* and V_p/*F*; V_c/*F*, apparent central volume of distribution; V_p/*F*, apparent peripheral volume of distribution; WT, total body weight.

IMPDH inhibition in paediatric kidney transplant patients. This is the first study using a population approach to link MPA PK to IMPDH inhibitory effects.

Although clinical target ranges for IMPDH inhibition to achieve desired efficacy are currently undefined, an increasing amount of evidence has demonstrated IMPDH activity as a reliable predictor of rejection episodes [2, 3, 15, 24, 25]. The potential benefit of an IMPDH activity based over a MPA concentration based MMF dosing strategy was supported by a recent clinical trial where IMPHD activity but not the MPA concentrations correlated with rejection episodes after renal transplantation [24]. Our study provided quantitative insight into the PK–PD relationship of MPA. The relationship between MPA concentration and IMPDH enzyme activity was well described by an inhibitory E_{max} model in this study. The population average EC_{50} of 1.73 mg l^{-1} was in good agreement with a previously reported value of 1.3–2.1 mg l^{-1} in liver transplantation patients [26]. Previously, baseline IMPDH activity (E_0) was suggested to correlate with clinical outcome [2]. High pre-transplant IMPDH activity is associated with high rejection rate whereas patients with a low IMPDH baseline value experience more adverse events. A recent report showed that an average of 50% IMPDH inhibition may be a good target level for preventing acute rejection episodes [24]. In the referred study, the group with an average IMPDH inhibition of 56.7% had no biopsy-proven rejection, whereas the group with acute rejection episodes had a significantly lower average percentage inhibition of IMPDH (26%). Further prospective clinical studies in aiming to determine the relationship between clinical outcome and IMPDH inhibition are warranted to further define the clinical target and verify whether the suggested 50% IMPDH inhibition would be optimal for better efficacy and lower toxicity. Consistent with an earlier study [25], we did not find any age-dependent difference in IMPDH activity in our small cohort of paediatric patients. However, African-American patients appeared to have a lower baseline IMPDH activity (E_0) than Caucasian patients. As only two African-American patients were included in our study cohort, a larger follow-up study is required to confirm these results. Our study also identified a marginal predictive effect of albumin on IMPDH baseline activity. With higher albumin concentrations, a lower free fraction would result in higher levels of IMPDH activity.

Mycophenolate PK are well known for their high inter-individual and intra-individual variability, especially the complex absorption [27]. For this reason, significant efforts

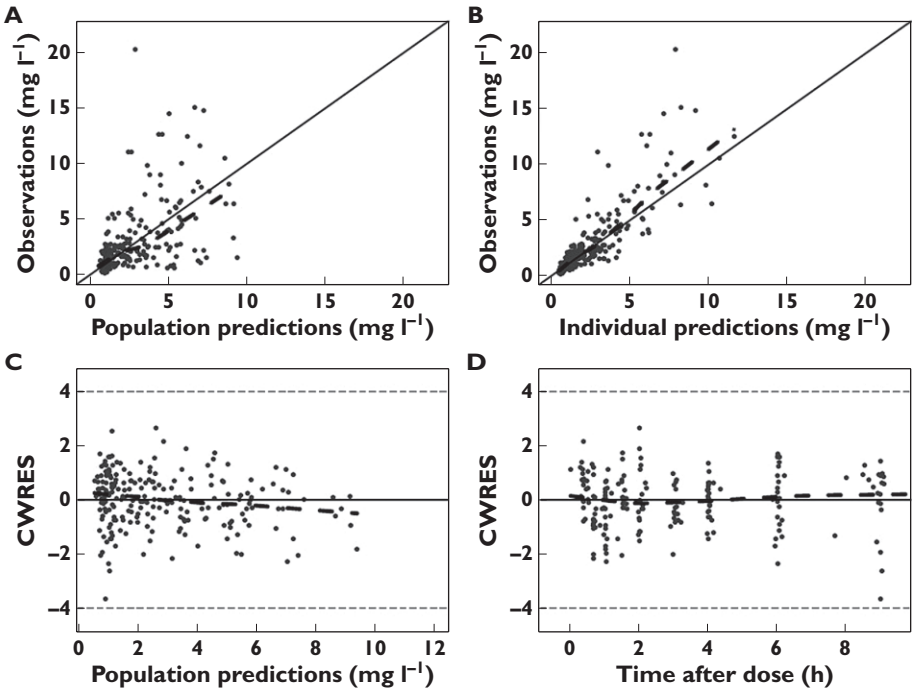

Figure 2

Goodness-of-fit plots for the final PK model. (A) Population prediction *vs.* observed concentration. (B) Individual prediction *vs.* observed concentration. (C) Conditional weighted residuals (CWRES) *vs.* population prediction. (D) Conditional weighted residuals (CWRES) *vs.* time after dose. Dashed line, a locally weighted least-squares regression; solid line, line of identity

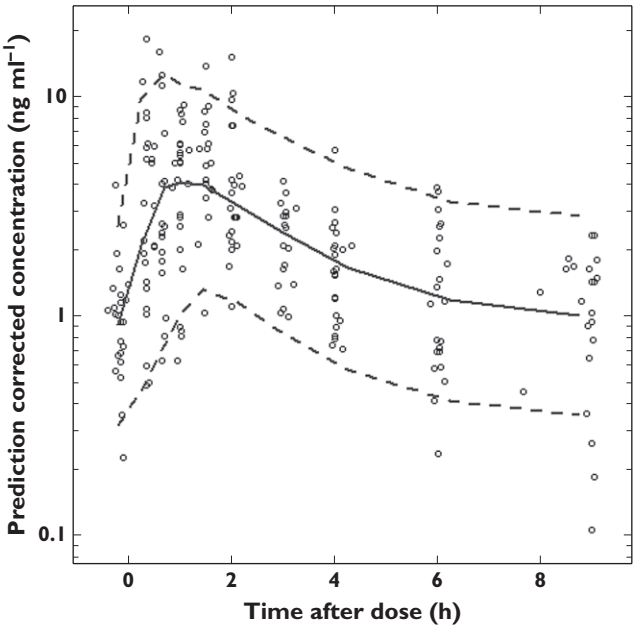

Figure 3

Prediction corrected visual predictive check (pcVPC) of the final model describing the population PK of MPA. Open circles, observed plasma concentrations; black lines represent the median, 5th and 95th percentiles of the simulated data ($n = 1000$). Plasma concentrations of MPA was plotted using a logarithmic (base 10) *y* axis

have been made to describe MPA absorption using various models, such as first order absorption with lag time and Erlang distribution models [7, 9, 28]. Our group is one of the first to apply a semi-mechanistic transit compartment model to describe variable absorption of MPA. As the advantages and caveats of the transit model have been discussed in recent publications [17, 18, 29], this approach has provided more flexibility to delineate the delay and onset of absorption with higher probability to capture better the maximum concentration than with more traditional absorption models.

The estimated population values of MPA CL/*F*, V_c/F and Q/*F* in our model were well aligned with previous studies [27, 30]. However, the V_p/F estimation of 411 l was higher than a previously reported value of 158 l in paediatric renal transplant patients [9]. We noticed that the majority of patients in that study did not have samples taken between 3 to 12 h after MMF administration, whereas most of our patients were sampled at 4, 6 and 9 h after-dose. It is possible that the reabsorption of MPA due to enterohepatic recycling was better captured in our study which may have contributed to the higher V_p/F estimate.

Recently, de Winter *et al*. [23] reported a non-linear relationship between MMF dose and exposure in adult renal transplant recipients, showing decreasing bioavailability with increasing dose. Drug non-proportionality was also observed in our paediatric

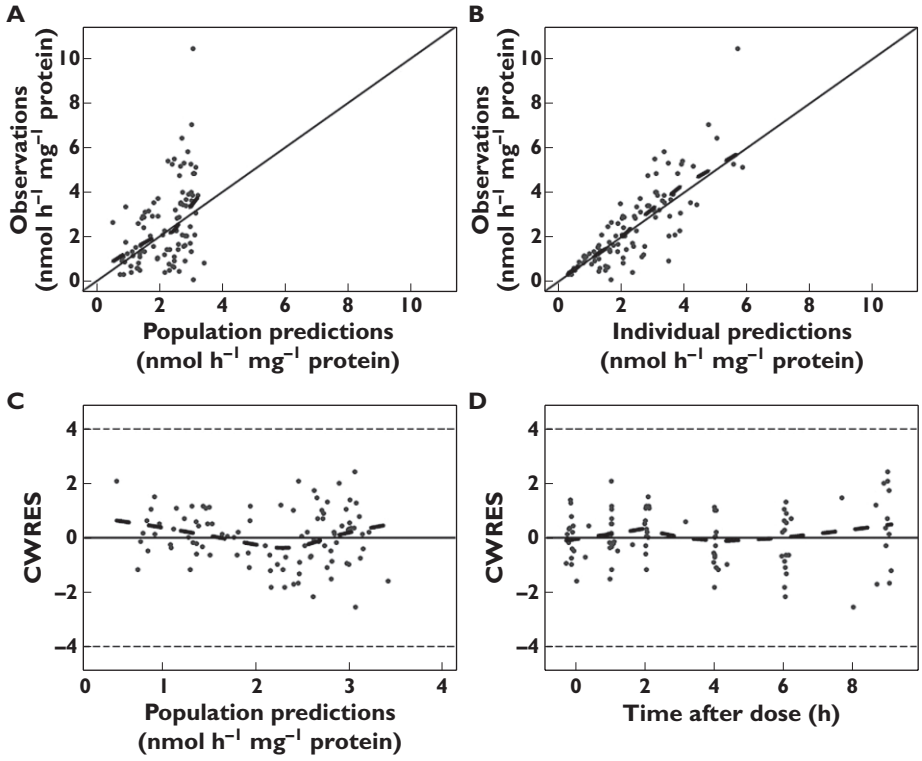

Figure 4

Goodness-of-fit plots for the final PK–PD model. (A) Population prediction *vs.* observed IMPDH activity. (B) Individual prediction *vs.* observed IMPDH activity. (C) Conditional weighted residuals (CWRES) *vs.* population prediction. (D) Conditional weighted residuals (CWRES) *vs.* time after dose. Dashed line, a locally weighted least-squares regression; solid line, line of identity

Table 3

Parameter estimates from the final PK–PD model and bootstrap analysis

Parameters	Final estimates	Shrinkage (%)	Bootstrap estimates*	
			Median	95% CI
E_0 (nmol h^{-1} mg^{-1} protein)	3.45		3.48	2.61, 4.56
EC_{50} (mg l^{-1})	1.73		1.73	1.16, 3.01
E_{max} (nmol h^{-1} mg^{-1} protein)	0 fix		–	–
Inter-individual variability (%CV)†				
ω (E_0)	39.6	13%	37.8	9.6, 56.2
ω (EC_{50})	72.5	26%	76.3	18.1, 152.5
ω (E_{max})	0 fix		–	–
Proportional residual error (%CV)[c]				
σ^{prop}	42.2	8%	41.7	34.6, 48.3

*Obtained from 220 out of 300 non-parametric bootstrap runs. †Reported as %CV, calculated by the equation 100*SQRT(exp(ω_n) – 1) where ω_n is the NONMEM output for the inter-subject variability of the *n* th parameter. [c]Calculated by the equation 100 × SQRT(σ), where σ is the NONMEM output for the variance of the proportional residual error. E_0 is the baseline IMPDH activity; E_{max} is the maximal fractional inhibitory effect; EC_{50} is the MPA concentration at half E_{max}; %CV: coefficient of variation; CI: confidence interval.

population (Figure 1) and was described by our model. Covariate analysis identified a power function of –0.43 between dose and relative bioavailability which is similar to the reported –0.41 for adults in de Winter's study. In clinical practice, this non-proportional relationship between dose and exposure should be taken into consideration when performing TDM. So far, no clear physiological explanation has been reported for this reduced bioavailability phenomenon although saturation of the absorption and of the enterohepatic circulation pathways have been suggested as possible causes [23].

Growth and developmental changes are the two main factors that influence drug PK in children. In population PK studies, it is now common practice to apply allometric

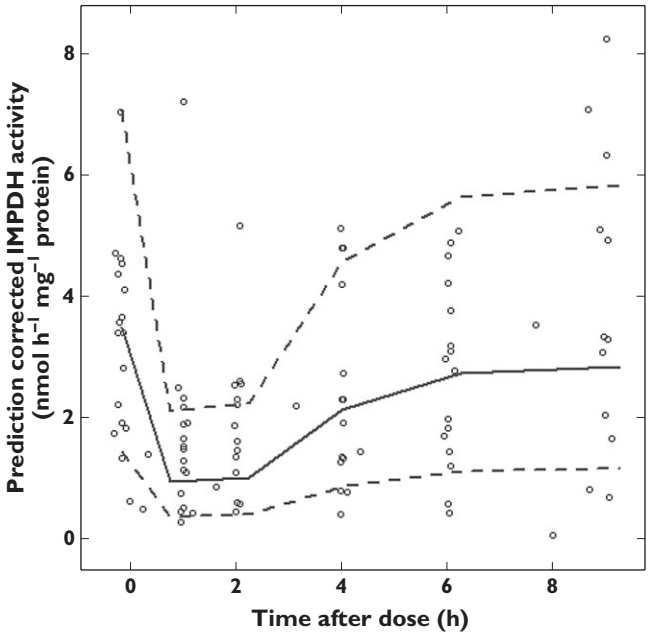

Figure 5

Prediction corrected visual predictive check (pcVPC) of the final model describing the population PK–PD model of MPA. Open circles, observed plasma concentrations; black lines represent the median, 5th and 95th percentiles of the simulated data ($n = 1000$)

scaling principles to clearance and volume parameters in paediatric studies [31]. However, we were not able to confirm a power exponent of 0.75 in the present study. Apparent clearance was found to correlate with allometrically scaled body weight with an exponent of only 0.31. Furthermore, weight was not shown to be a predicting factor of volume of distribution, nor of inter-compartmental clearance. Given that the goal for PK modelling in our study was to provide parameters to best describe PK data for the PK–PD model development, we therefore chose to use a more descriptive method rather than a more mechanistic/theoretical-based method. Interestingly, it is not unusual to see a low impact of body mass on the clearance of MPA in children. In a study performed in paediatric patients with an age range of 1.6–18.3 years, the exponent of body weight on MPA CL/*F* was 0.424 [9]. In another study, Le Guellec *et al*. identified total body weight as a contributing covariate on CL with a power exponent of 0.25 [32]. The reason of why our and other studies were not in agreement with the $^3/_4$ exponent law is unclear. A possible explanation is the highly variable MPA PK profile which may conceal the true relationship between body mass and clearance. Another explanation might be enterohepatic recirculation and variable bioavailability, as this complicates the estimation of 'true' oral clearance. In addition, there is ongoing debate related to the overall applicability of a fixed exponent of 0.75 to the prediction of drug clearance and several studies suggest a data driven approach to analyzing the relationship between body size measures and clearance, as was used in the current study [33–35].

Previous studies in adults and in children have identified many possible causes for between subject PK variability, including renal function [7, 36, 37], serum albumin [38, 39], co-medication [9, 23] and genetic polymorphisms in drug metabolizing enzymes [40, 41]. However, except for body weight, no other covariates were identified in this patient cohort. One reason could be the relative small sample size. Also, for some covariates such as albumin, the correlation with MPA clearance may be better manifested longitudinally within each individual patient due to large inter-individual variability of MPA drug exposure [42].

There are limitations to this study. Firstly, we did not include enterohepatic recirculation in the final model despite the fact that a significant amount can be reabsorbed through this mechanism. Reasons for this were the increased computational complexity and the fact that a relatively small number of patients presented with clear reabsorption or a secondary peak(s) attributable to enterohepatic recirculation. Secondly, MPA has high protein binding and it is postulated that only the free MPA concentration is pharmacologically active [43]. Although recent studies suggest that both total MPA and free MPA are equally good predictors of the immunosuppressive response [42, 44], it remains of interest to study further the dose proportionality, covariates effects and the relationship between drug exposure and effect of unbound MPA in more detail.

In summary, an integrated population PK–PD model of MPA has been developed in paediatric renal transplant recipients. The current model provides information that will facilitate future studies on guiding MPA treatment using a PK–PD based therapeutic drug management strategy.

Competing Interests

All authors have completed the Unified Competing Interest form at http://www.icmje.org/coi_disclosure.pdf (available on request from the corresponding author) and declare TF and AAV were partially supported by grants 5U10HD037249 (TF, AAV) and 5K24HD050387 (AAV) from the National Institutes of Health. There are no financial relationships with any organizations that might have an interest in the submitted work in the previous 3 years and no other relationships or activities that could appear to have influenced the submitted work.

This work was in part supported by grants 5U10HD037249 (TF, AAV) and 5K24HD050387 (AAV) from the National Institutes of Health and an investigator initiated research grant (AAV) from Roche Laboratories, Inc (Nutley, New Jersey). We thank colleagues Joseph Sherbotie, MD, Mouin Seikaly, MD, George McCracken, MD, Laura James, MD

and Robert Ward, MD, and their staff in the Pediatric Pharmacology Research Unit network for their support with the collection of the data. We thank Drs Radojka Savic and Justin Wilkins for their valuable suggestions and comments on the application of the transit compartment absorption model.

REFERENCES

1 Tonshoff B, David-Neto E, Ettenger R, Filler G, van Gelder T, Goebel J, Kuypers DR, Tsai E, Vinks AA, Weber LT, Zimmerhackl LB. Pediatric aspects of therapeutic drug monitoring of mycophenolic acid in renal transplantation. Transplant Rev (Orlando) 2011; 25: 78–89.

2 Glander P, Hambach P, Braun KP, Fritsche L, Giessing M, Mai I, Einecke G, Waiser J, Neumayer HH, Budde K. Pre-transplant inosine monophosphate dehydrogenase activity is associated with clinical outcome after renal transplantation. Am J Transplant 2004; 4: 2045–51.

3 Fukuda T, Goebel J, Thogersen H, Maseck D, Cox S, Logan B, Sherbotie J, Seikaly M, Vinks AA. Inosine monophosphate dehydrogenase (IMPDH) activity as a pharmacodynamic biomarker of mycophenolic acid effects in pediatric kidney transplant recipients. J Clin Pharmacol 2011; 51: 309–20.

4 Weimert NA, Derotte M, Alloway RR, Woodle ES, Vinks AA. Monitoring of inosine monophosphate dehydrogenase activity as a biomarker for mycophenolic acid effect: potential clinical implications. Ther Drug Monit 2007; 29: 141–9.

5 Le Meur Y, Buchler M, Thierry A, Caillard S, Villemain F, Lavaud S, Etienne I, Westeel PF, Hurault de Ligny B, Rostaing L, Thervet E, Szelag JC, Rerolle JP, Rousseau A, Touchard G, Marquet P. Individualized mycophenolate mofetil dosing based on drug exposure significantly improves patient outcomes after renal transplantation. Am J Transplant 2007; 7: 2496–503.

6 Kuypers DR, Le Meur Y, Cantarovich M, Tredger MJ, Tett SE, Cattaneo D, Tonshoff B, Holt DW, Chapman J, Gelder T. Consensus report on therapeutic drug monitoring of mycophenolic acid in solid organ transplantation. Clin J Am Soc Nephrol 2010; 5: 341–58.

7 Kim H, Long-Boyle J, Rydholm N, Orchard PJ, Tolar J, Smith AR, Jacobson P, Brundage R. Population pharmacokinetics of unbound mycophenolic acid in pediatric and young adult patients undergoing allogeneic hematopoietic cell transplantation. J Clin Pharmacol 2012; 52: 1665–75.

8 Premaud A, Le Meur Y, Debord J, Szelag JC, Rousseau A, Hoizey G, Toupance O, Marquet P. Maximum a posteriori bayesian estimation of mycophenolic acid pharmacokinetics in renal transplant recipients at different postgrafting periods. Ther Drug Monit 2005; 27: 354–61.

9 Zhao W, Fakhoury M, Deschenes G, Roussey G, Brochard K, Niaudet P, Tsimaratos M, Andre JL, Cloarec S, Cochat P, Bensman A, Azougagh S, Jacqz-Aigrain E. Population pharmacokinetics and pharmacogenetics of mycophenolic acid following administration of mycophenolate mofetil in de novo pediatric renal-transplant patients. J Clin Pharmacol 2010; 50: 1280–91.

10 Staatz CE, Tett SE. Maximum *a posteriori* Bayesian estimation of mycophenolic Acid area under the concentration-time curve: is this clinically useful for dosage prediction yet? Clin Pharmacokinet 2011; 50: 759–72.

11 Klupp J, Holt DW, van Gelder T. How pharmacokinetic and pharmacodynamic drug monitoring can improve outcome in solid organ transplant recipients. Transpl Immunol 2002; 9: 211–4.

12 Peters AM, Snelling HL, Glass DM, Bird NJ. Estimation of lean body mass in children. Br J Anaesth 2011; 106: 719–23.

13 Duffull SB, Dooley MJ, Green B, Poole SG, Kirkpatrick CM. A standard weight descriptor for dose adjustment in the obese patient. Clin Pharmacokinet 2004; 43: 1167–78.

14 Schwartz GJ, Haycock GB, Edelmann CM Jr, Spitzer A. A simple estimate of glomerular filtration rate in children derived from body length and plasma creatinine. Pediatrics 1976; 58: 259–63.

15 Glander P, Sombogaard F, Budde K, van Gelder T, Hambach P, Liefeldt L, Lorkowski C, Mai M, Neumayer HH, Vulto AG, Mathot RA. Improved assay for the nonradioactive determination of inosine 5′-monophosphate dehydrogenase activity in peripheral blood mononuclear cells. Ther Drug Monit 2009; 31: 351–9.

16 Holford NH, Ambros RJ, Stoeckel K. Models for describing absorption rate and estimating extent of bioavailability: application to cefetamet pivoxil. J Pharmacokinet Biopharm 1992; 20: 421–42.

17 Savic RM, Jonker DM, Kerbusch T, Karlsson MO. Implementation of a transit compartment model for describing drug absorption in pharmacokinetic studies. J Pharmacokinet Pharmacodyn 2007; 34: 711–26.

18 Wilkins JJ, Savic RM, Karlsson MO, Langdon G, McIlleron H, Pillai G, Smith PJ, Simonsson US. Population pharmacokinetics of rifampin in pulmonary tuberculosis patients, including a semimechanistic model to describe variable absorption. Antimicrob Agents Chemother 2008; 52: 2138–48.

19 Lindbom L, Ribbing J, Jonsson EN. Perl-speaks-NONMEM (PsN)-a Perl module for NONMEM related programming. Comput Methods Programs Biomed 2004; 75: 85–94.

20 Bergstrand M, Hooker AC, Wallin JE, Karlsson MO. Prediction-corrected visual predictive checks for diagnosing nonlinear mixed-effects models. AAPS J 2011; 13: 143–51.

21 Karlsson MO, Savic RM. Diagnosing model diagnostics. Clin Pharmacol Ther 2007; 82: 17–20.

22 Sherwin CM, Sagcal-Gironella AC, Fukuda T, Brunner HI, Vinks AA. Development of population PK model with enterohepatic circulation for mycophenolic acid in patients with childhood-onset systemic lupus erythematosus. Br J Clin Pharmacol 2012; 73: 727–40.

23 de Winter BC, Mathot RA, Sombogaard F, Vulto AG, van Gelder T. Nonlinear relationship between mycophenolate mofetil dose and mycophenolic acid exposure: implications for therapeutic drug monitoring. Clin J Am Soc Nephrol 2011; 6: 656–63.

24 Raggi MC, Siebert SB, Steimer W, Schuster T, Stangl MJ, Abendroth DK. Customized mycophenolate dosing based on measuring inosine-monophosphate dehydrogenase activity significantly improves patients' outcomes after renal transplantation. Transplantation 2010; 90: 1536–41.

25 Rother A, Glander P, Vitt E, Czock D, von Ahsen N, Armstrong VW, Oellerich M, Budde K, Feneberg R, Tonshoff B, Weber LT. Inosine monophosphate dehydrogenase activity in paediatrics: age-related regulation and response to mycophenolic acid. Eur J Clin Pharmacol 2012; 68: 913–22.

26 Premaud A, Rousseau A, Johnson G, Canivet C, Gandia P, Muscari F, Peron JM, Rostaing L, Marquet P, Kamar N. Inhibition of T-cell activation and proliferation by mycophenolic acid in patients awaiting liver transplantation: PK/PD relationships. Pharmacol Res 2011; 63: 432–8.

27 Sherwin CM, Fukuda T, Brunner HI, Goebel J, Vinks AA. The evolution of population pharmacokinetic models to describe the enterohepatic recycling of mycophenolic acid in solid organ transplantation and autoimmune disease. Clin Pharmacokinet 2011; 50: 1–24.

28 Saint-Marcoux F, Royer B, Debord J, Larosa F, Legrand F, Deconinck E, Kantelip JP, Marquet P. Pharmacokinetic modelling and development of Bayesian estimators for therapeutic drug monitoring of mycophenolate mofetil in reduced-intensity haematopoietic stem cell transplantation. Clin Pharmacokinet 2009; 48: 667–75.

29 Shen J, Boeckmann A, Vick A. Implementation of dose superimposition to introduce multiple doses for a mathematical absorption model (transit compartment model). J Pharmacokinet Pharmacodyn 2012; 39: 251–62.

30 Dong M, Fukuda T, Vinks AA. Optimization of mycophenolic acid therapy using clinical pharmacometrics. Drug Metab Pharmacokinet 2014; 29: 4–11.

31 Anderson BJ, Holford NH. Tips and traps analyzing pediatric PK data. Paediatr Anaesth 2011; 21: 222–37.

32 Le Guellec C, Bourgoin H, Buchler M, Le Meur Y, Lebranchu Y, Marquet P, Paintaud G. Population pharmacokinetics and Bayesian estimation of mycophenolic acid concentrations in stable renal transplant patients. Clin Pharmacokinet 2004; 43: 253–66.

33 Krekels EH, van Hasselt JG, Tibboel D, Danhof M, Knibbe CA. Systematic evaluation of the descriptive and predictive performance of paediatric morphine population models. Pharm Res 2011; 28: 797–811.

34 Mahmood I. Pharmacokinetic allometric scaling of antibodies: application to the first-in-human dose estimation. J Pharm Sci 2009; 98: 3850–61.

35 Kolokotrones T, Van S, Deeds EJ, Fontana W. Curvature in metabolic scaling. Nature 2010; 464: 753–6.

36 Frymoyer A, Verotta D, Jacobson P, Long-Boyle J. Population pharmacokinetics of unbound mycophenolic acid in adult allogeneic haematopoietic cell transplantation: effect of pharmacogenetic factors. Br J Clin Pharmacol 2013; 75: 463–75.

37 Sam WJ, Joy MS. Population pharmacokinetics of mycophenolic acid and metabolites in patients with glomerulonephritis. Ther Drug Monit 2010; 32: 594–605.

38 Li H, Mager DE, Sandmaier BM, Maloney DG, Bemer MJ, McCune JS. Population pharmacokinetics and dose optimization of mycophenolic acid in HCT recipients receiving oral mycophenolate mofetil. J Clin Pharmacol 2013; 53: 393–402.

39 Guillet BA, Simon NS, Purgus R, Botta C, Morange S, Berland Y, Pisano PS. Population pharmacokinetics analysis of mycophenolic acid in adult kidney transplant patients with chronic graft dysfunction. Ther Drug Monit 2010; 32: 427–32.

40 Prausa SE, Fukuda T, Maseck D, Curtsinger KL, Liu C, Zhang K, Nick TG, Sherbotie JR, Ellis EN, Goebel J, Vinks AA. UGT genotype may contribute to adverse events following medication with mycophenolate mofetil in pediatric kidney transplant recipients. Clin Pharmacol Ther 2009; 85: 495–500.

41 Zhao W, Elie V, Baudouin V, Bensman A, Andre JL, Brochard K, Broux F, Cailliez M, Loirat C, Jacqz-Aigrain E. Population pharmacokinetics and Bayesian estimator of mycophenolic acid in children with idiopathic nephrotic syndrome. Br J Clin Pharmacol 2010; 69: 358–66.

42 Smits TA, Cox S, Fukuda T, Sherbotie J, Ward R, Goebel J, Vinks AA. The effects of unbound mycophenolic acid (MPA) on inosine monophosphate dehydrogenase (IMPDH) inhibition in pediatric kidney transplant patients. Ther Drug Monit 2014. [Epub ahead of print].

43 Nowak I, Shaw LM. Mycophenolic acid binding to human serum albumin: characterization and relation to pharmacodynamics. Clin Chem 1995; 41: 1011–7.

44 Reine PA, Vethe NT, Kongsgaard UE, Andersen AM, Line PD, Ali AM, Bergan S. Mycophenolate pharmacokinetics and inosine monophosphate dehydrogenase activity in liver transplant recipients with an emphasis on therapeutic drug monitoring. Scand J Clin Lab Invest 2013; 73: 117–24.